THE OHIO STATE UNIVERSITY

MACHINE LEARNING BASED INTERACTION FORCE AND COLLISION MODELS FOR IRREGULAR SHAPED PARTICLES IN GAS-SOILD FLOWS

Soohwan Hwang, Jianhua Pan, and Liang-Shih Fan

Gas-Solid system

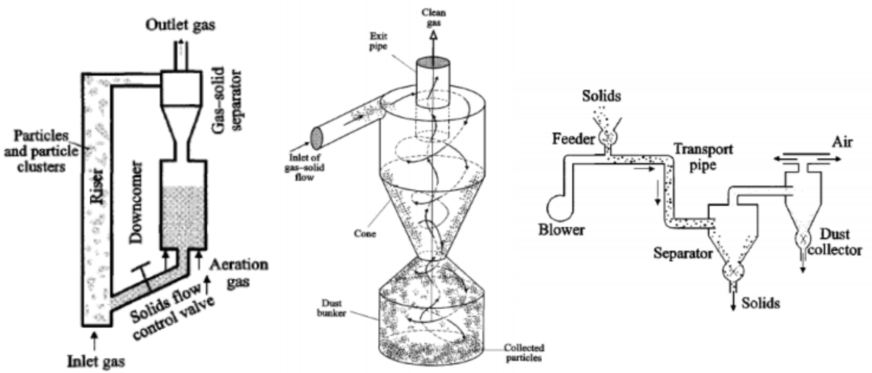

Interaction forces

DNS

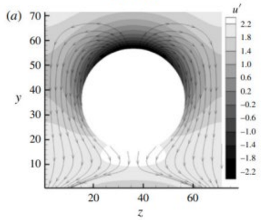

Fluidized bed

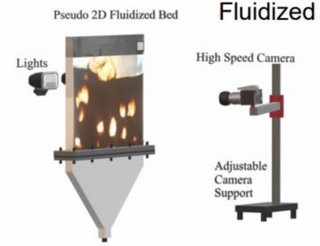

Machine Learning

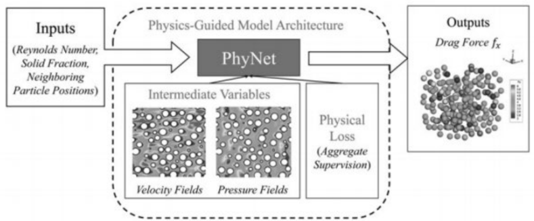

Liang-Shih Fan, Principles of gas-solid flows (1999)

Qiang Zhou et al., Journal of Fluid Mechanics, 765 (2015)

Cesar Martin Venier et al. International Journal of Numerical Methods for Heat and Fluid Flow

Long He et al., Powder Technology 345 (2019)

Irregular shaped particles

- Require to involve complicated geometrical factors sphericity, flatness, elongation and circularity, etc.
- Most force correlations are limited to simplified or regular shaped particle
- Require heavy computation for the collision
- Neural network approach
- Interaction force: Drag, lifting, Torque
- Collision contact properties: Contact point, norm, inter-penetration depth

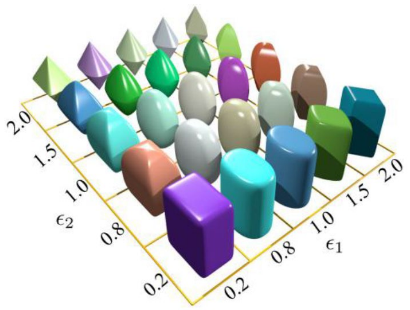

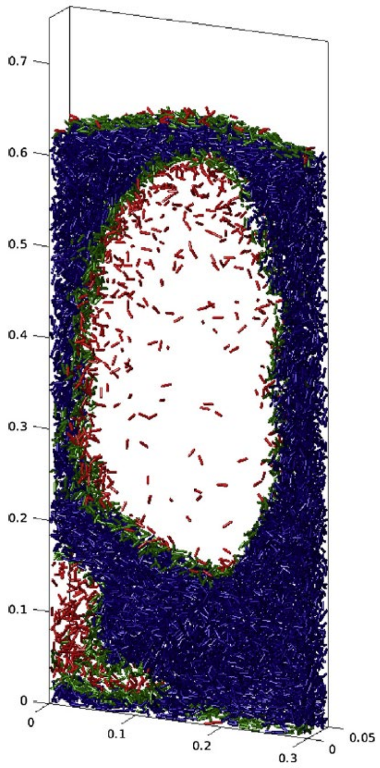

Shiwei Zhao et al., Int J Numer Anal Methods Geomech., 43 (2019)

Vinay V. Mahajan et al., Chemical Engineering Science, 192 (2018)

Interaction Force Model

Background

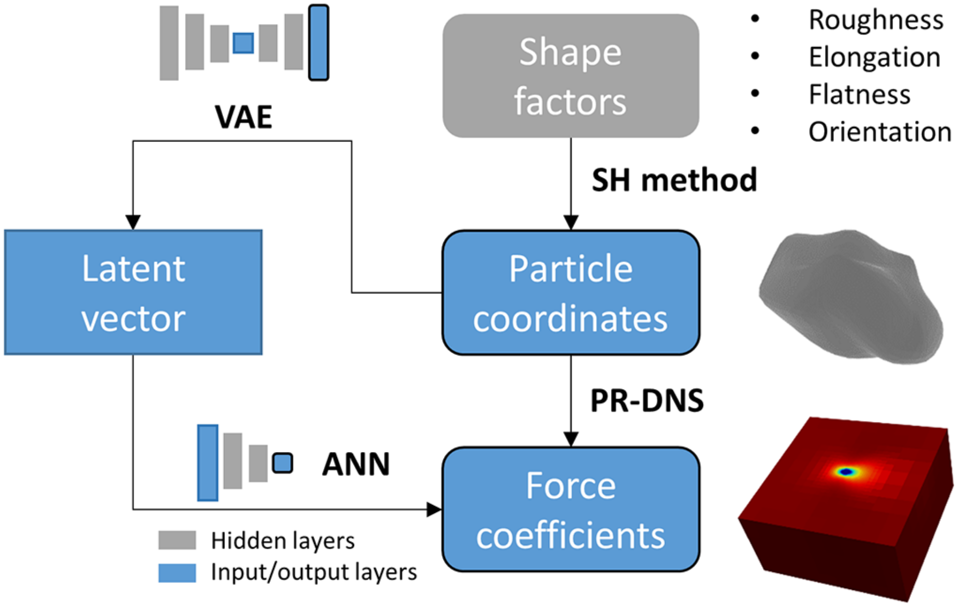

Irregular shaped

A single fixed particle in low *Re* flow

SH : Spherical Harmonic method
VAE : Variational Auto-Encoder
PR-DNS : Particle Resolved Direct Numerical Simulation
ANN : Artificial Neural Network

Spherical Harmonic (SH) Method

- Spherical harmonic functions

$$\begin{pmatrix} x(\theta,\phi) \\ y(\theta,\phi) \\ z(\theta,\phi) \end{pmatrix} = \begin{pmatrix} \sum_{l=1}^{l_{max}} \sum_{m=-l}^{l} C_{x,l}^{m} Y_l^m(\theta,\phi) \\ \sum_{l=1}^{l_{max}} \sum_{m=-l}^{l} C_{y,l}^{m} Y_l^m(\theta,\phi) \\ \sum_{l=1}^{l_{max}} \sum_{m=-l}^{l} C_{z,l}^{m} Y_l^m(\theta,\phi) \end{pmatrix}$$

- Few shape factors
  - d : spherical descriptor, roughness
  - EI : elongation index
  - FI : flatness index
- Randomness, $C_l = f_l(d, X \sim U(0,1))$

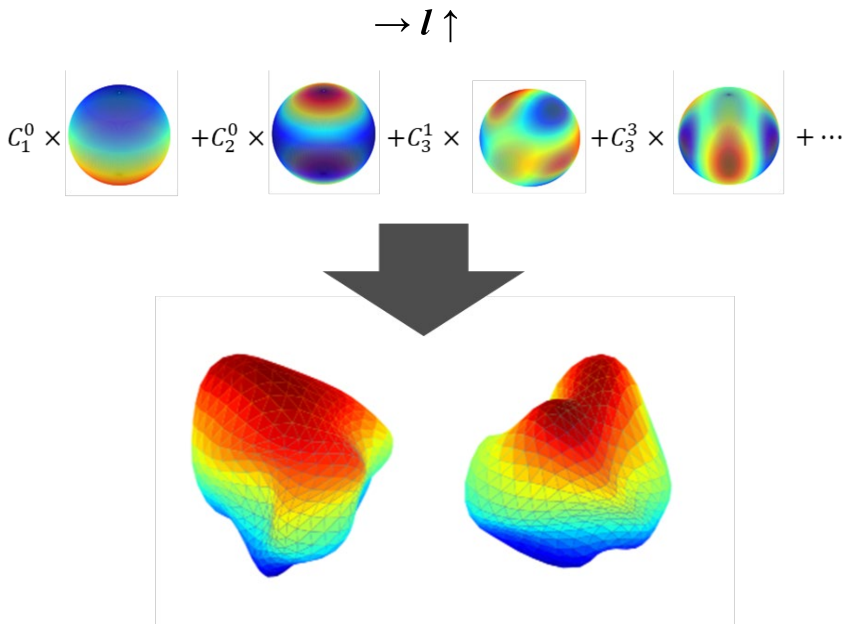

$d = 0.5,\ FI = 1,\ EI = 1$

Variational Auto-Encoder (VAE)

- Voxel input
- Deep CNN layers with ELUs
- Latent vectors with 128 dimension
- 2,000 datasets to train, 400 datasets to validate
- Less than 1% reconstruction error
- For the DNS, new 5,200 particles were generated (error < 1%)

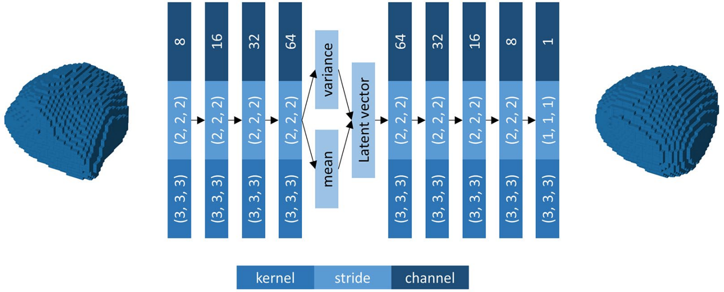

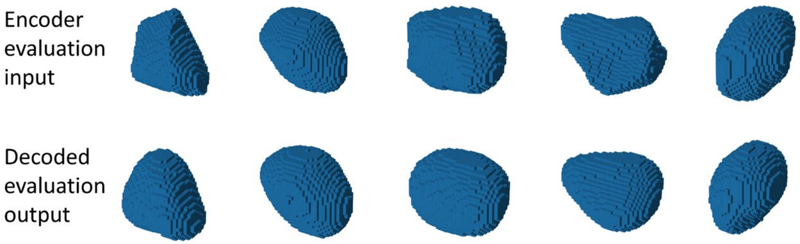

PR-DNS Development

- Simplified Spheric Gas Kinetic Scheme (GKS)
- Immersed boundary Method (IBM) / Direct Forcing
- Adaptive Mesh Refinement (AMR)

$$\frac{\partial f}{\partial t} + v \cdot \nabla f = \frac{g-f}{\tau}$$

$$f(0,t) \approx g(0,t) + \frac{\tau}{\delta t}\left(g(-v\delta t, t-\delta t) + g(0,t)\right)$$

$$\boldsymbol{F} = \int f(0,t) v_x \boldsymbol{\Xi} d\boldsymbol{v} \ , \ \boldsymbol{\Xi} = \begin{pmatrix} 1 \\ \boldsymbol{v} \end{pmatrix}$$

$$\frac{\partial \boldsymbol{W}}{\partial t} + \nabla \cdot \boldsymbol{F} = 0, \ \boldsymbol{W} = \begin{pmatrix} \rho \\ \rho \boldsymbol{u} \end{pmatrix}$$

$$g = \begin{cases} \frac{\rho}{4\pi}, & if \ (\boldsymbol{u} - \boldsymbol{v})^2 = c^2 \\ 0, & otherwise \end{cases}$$

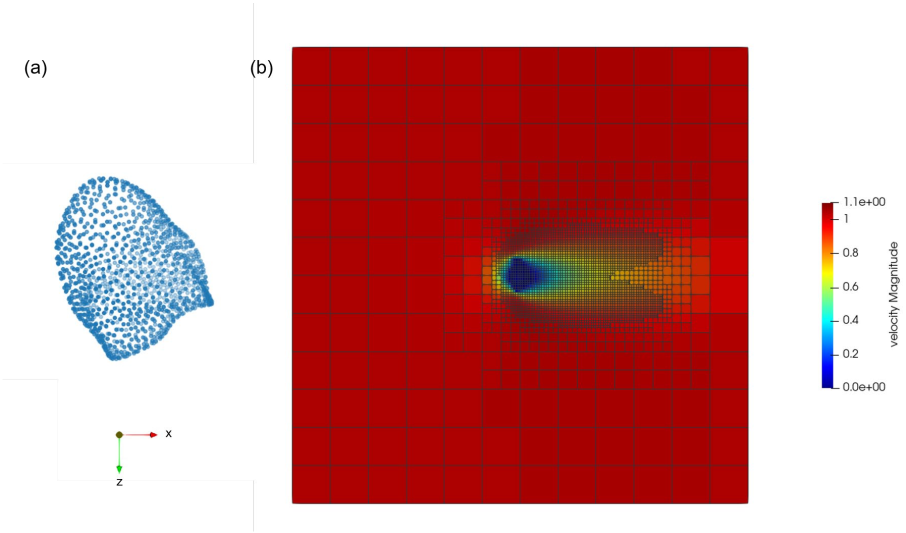

DNS to ANN

- 5,200 datasets in low Re regime (0.1~10)
- Show the typical Re-C_d trend, C_d and C_t depend on d, C_l depends on AR
- 1,000~4,000 datasets for training and 1,200 datasets for validation and evaluation

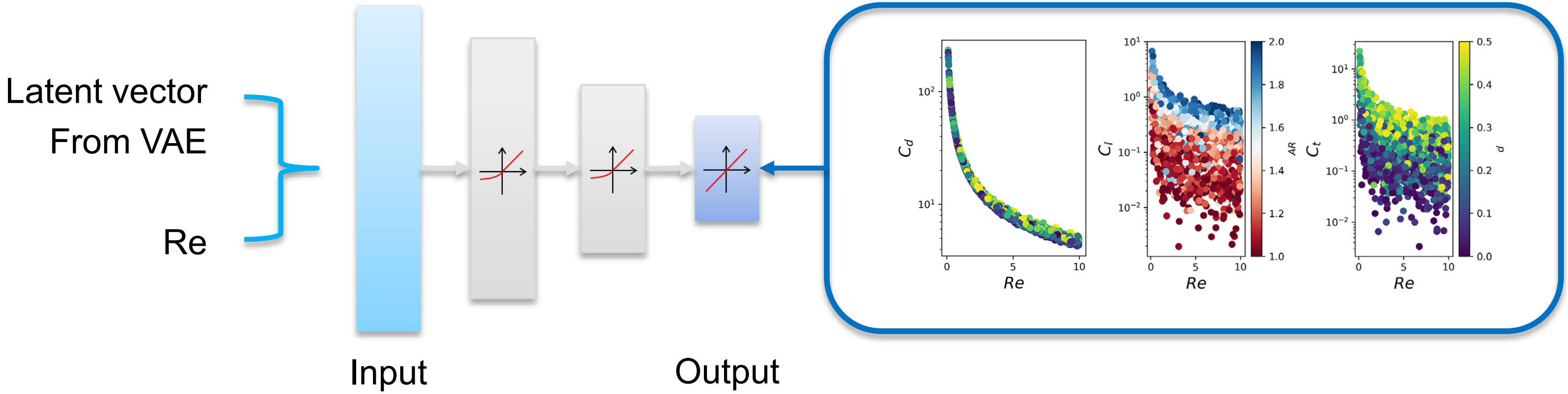

ANN results

- MSEs for eq (1) is 21.8 which is comparable to the ANN result (12.7±2.7)
- MAPE of C_d is 4.5% which is lower than 11.8% from eq (1)

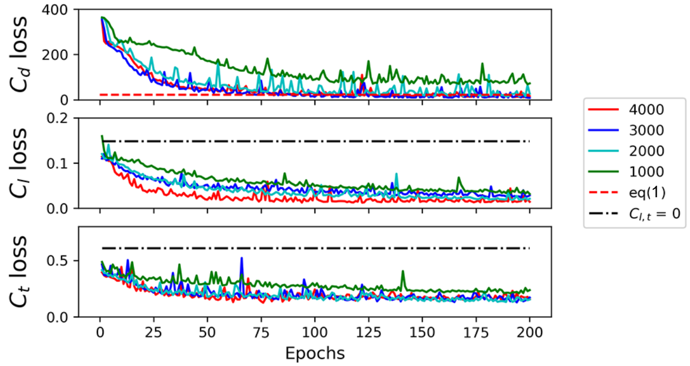

$$C_d = \frac{24}{ReK_1}\{1 + 0.1118(ReK_1K_2)^{0.6567}\} + \frac{0.4305K_2}{1+\frac{3305}{ReK_1K_2}} \quad (1)$$

$$K_1 = [\left(\frac{d_n}{3D_{eq}}\right) + 2/3\psi^{-0.5}]^{-1},\ K_2 = 10^{1.8148(-log\psi)^{0.5743}}$$

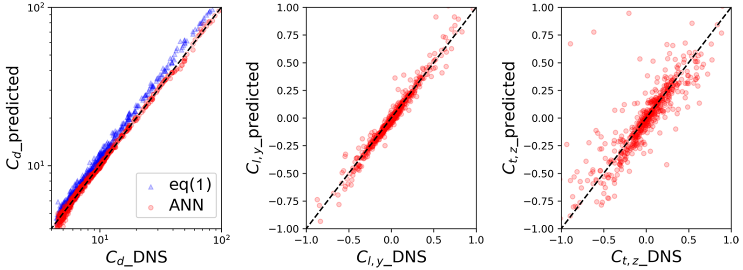

G.H. Ganser, Powder Technology. 77 (1993)

ANN results

- 3 particles (*d* = 0, 0.25, 0.5)
- More accurate prediction on the lifting force and torque coefficients.

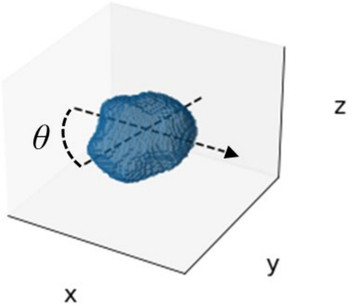

$$C_d = \frac{a_1}{Re^{a_2}} + \frac{a_3}{Re^{a_4}} + \left(\frac{a_5}{Re^{a_6}} + \frac{a_7}{Re^{a_8}} - \frac{a_1}{Re^{a_2}} - \frac{a_3}{Re^{a_4}}\right)sin(\theta)^{a_9}$$

$$C_l = \left(\frac{b_1}{Re^{b_2}} + \frac{b_3}{Re^{b_4}}\right)sin(\theta)^{b_5+b_6Re^{b_7}}cos(\theta)^{b_8+b_9Re^{b_{10}}} \qquad (2)$$

$$C_t = \left(\frac{c_1}{Re^{c_2}} + \frac{c_3}{Re^{c_4}}\right)sin(\theta)^{c_5+c_6Re^{c_7}}cos(\theta)^{c_8+c_9Re^{c_{10}}}$$

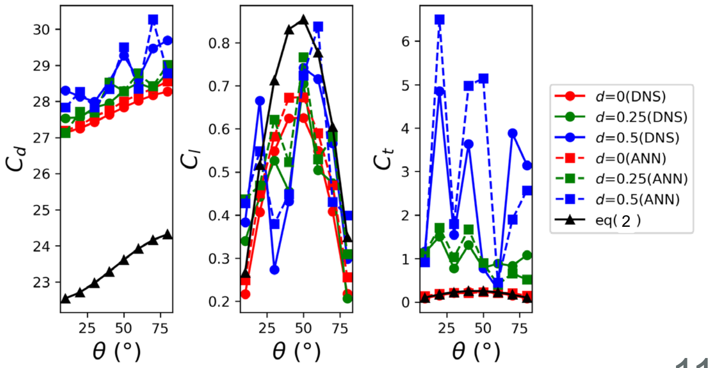

M. Zastawny, el al., International Journal of Multiphase Flow. 39 (2012)

Collision Model

Collision algorithms in CFD-DEM

- DEM method involves iterative calculations for particles

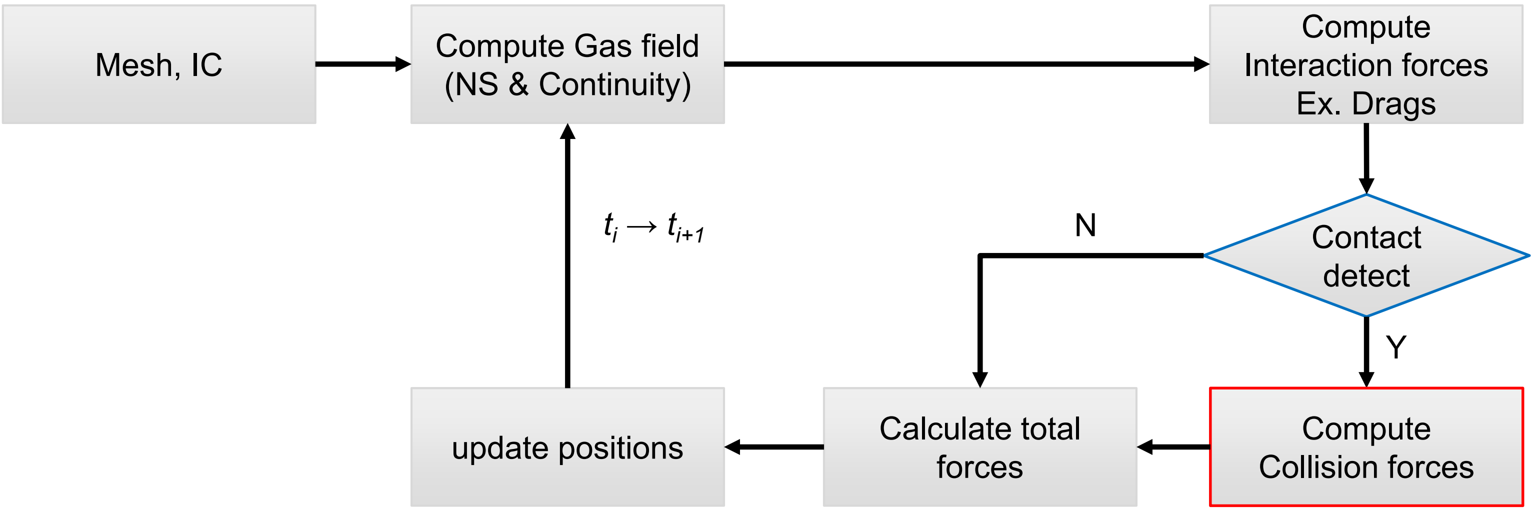

Collision algorithms in CFD-DEM

- At $t = t_i$ *and for* j^{th} *particle,*

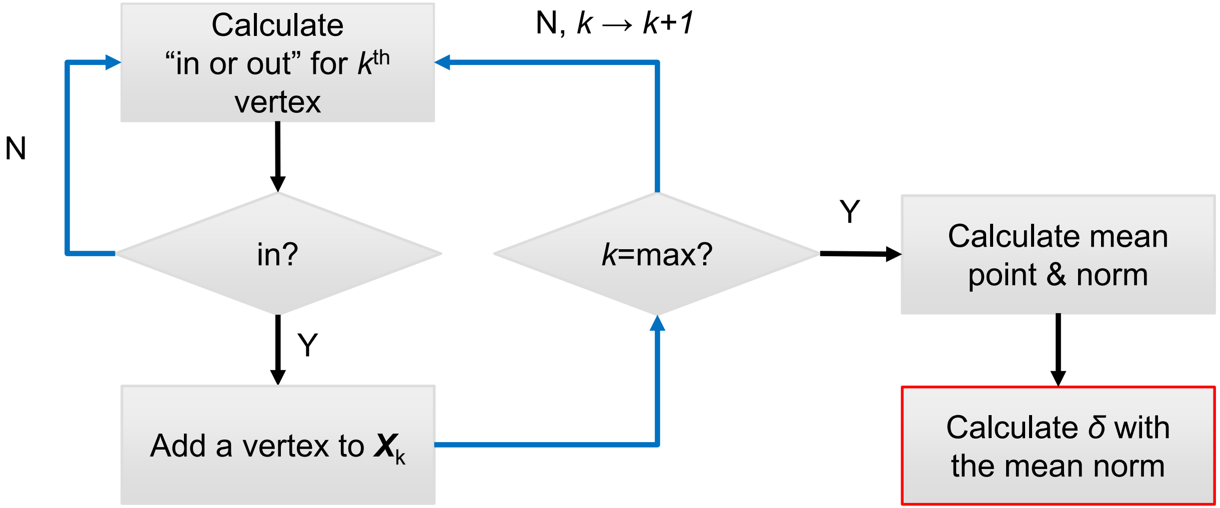

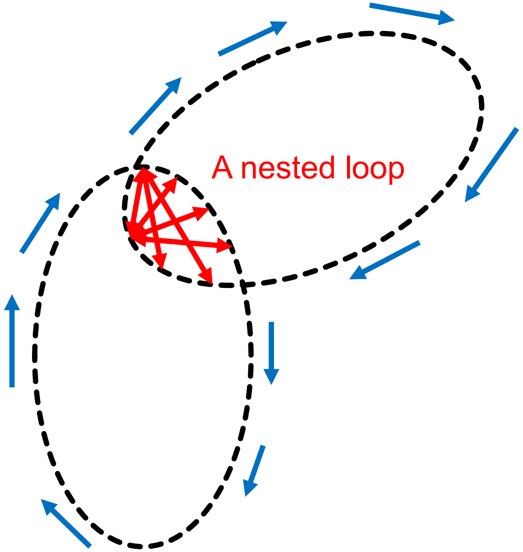

Non-spherical particles

- Regular & irregular particles

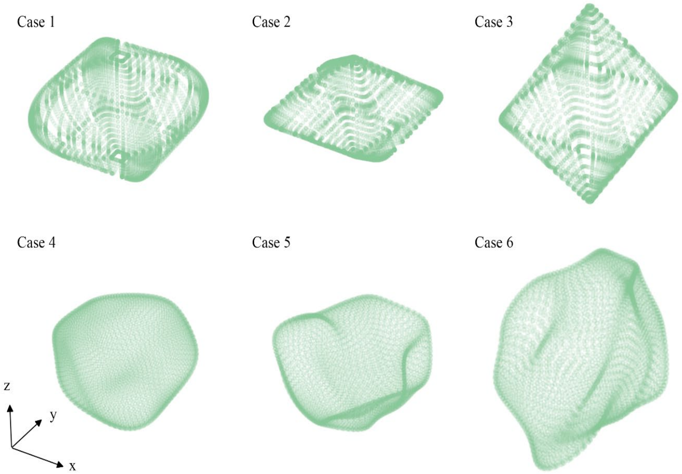

$$\left(\left(\frac{x}{r_1}\right)^{2/\varepsilon_1}+\left(\frac{y}{r_2}\right)^{2/\varepsilon_1}\right)^{\varepsilon_1/\varepsilon_2}+\left(\frac{z}{r_3}\right)^{2/\varepsilon_1}=1$$

$$x = r_1 sign(cos\varphi_1)|cos\varphi_1|^{\varepsilon_1}|cos\varphi_2|^{\varepsilon_2}$$

$$y = r_2 sign(sin\varphi_1)|sin\varphi_1|^{\varepsilon_1}|cos\varphi_2|^{\varepsilon_2}$$

$$z = r_3 sign(sin\varphi_2)|sin\varphi_2|^{\varepsilon_2}$$

$$\dot{x}=\frac{2}{\varepsilon_2}\left(\left|\frac{x}{r_1}\right|^{\frac{2}{\varepsilon_1}}+\left|\frac{y}{r_2}\right|^{\frac{2}{\varepsilon_1}}\right)^{\frac{\varepsilon_1-\varepsilon_2}{\varepsilon_1}}|x|^{\frac{2-\varepsilon_1}{\varepsilon_1}}|r_1|^{-\frac{2}{\varepsilon_1}}$$

$$\dot{y}=\frac{2}{\varepsilon_2}\left(\left|\frac{x}{r_1}\right|^{\frac{2}{\varepsilon_1}}+\left|\frac{y}{r_2}\right|^{\frac{2}{\varepsilon_1}}\right)^{\frac{\varepsilon_1-\varepsilon_2}{\varepsilon_1}}|y|^{\frac{2-\varepsilon_1}{\varepsilon_1}}|r_2|^{-\frac{2}{\varepsilon_1}}$$

$$\dot{z}=\frac{2}{\varepsilon_2}|z|^{\frac{2-\varepsilon_2}{\varepsilon_2}}|r_3|^{-\frac{2}{\varepsilon_2}}$$

$$\tilde{\boldsymbol{n}}=(n_x,n_y,n_z)=\frac{\boldsymbol{n}}{|\boldsymbol{n}|}=\frac{1}{2|\boldsymbol{n}|}\left(\frac{1}{N_1}\sum_{i=1}^{N_1}\dot{\boldsymbol{X}}_{1,i}\frac{A_{1,i}}{A_1}+\frac{1}{N_2}\sum_{j=1}^{N_2}\dot{\boldsymbol{X}}_{2,j}\frac{A_{2,j}}{A_2}\right)$$

ANN model

- Correlate the relative position, rotational angle and vertices to contact properties.
- Two ANN models for the detection and to properties.

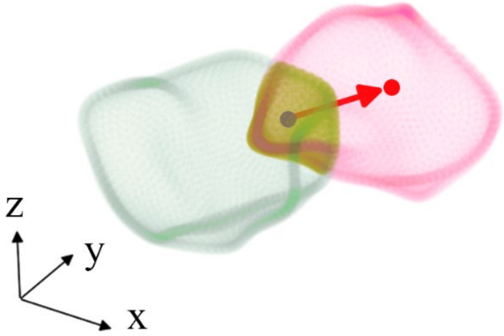

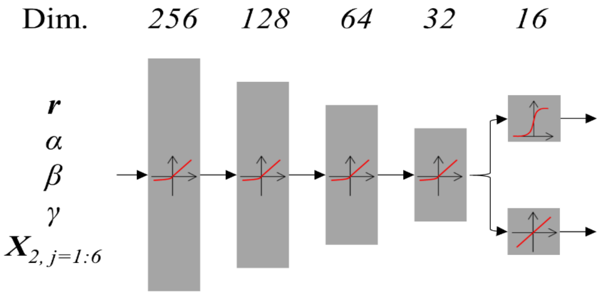

Contact detection : True/False $H_p(q) = -\frac{1}{N}\sum_{i=1}^{N} y_i \cdot log(p(y_i)) + (1-y_i)\cdot log(1-p(y_i))$

Contact calculation : $\boldsymbol{X}_{mean}$, $\tilde{\boldsymbol{n}}$, δ $\mathrm{MSE} = \frac{1}{n}\sum_{i=1}^{n}(Y_i - \hat{Y}_i)^2$

ANN results

- 80,000 datasets
- More accurate prediction compared to volume equivalent sphere
- Rapid calculations

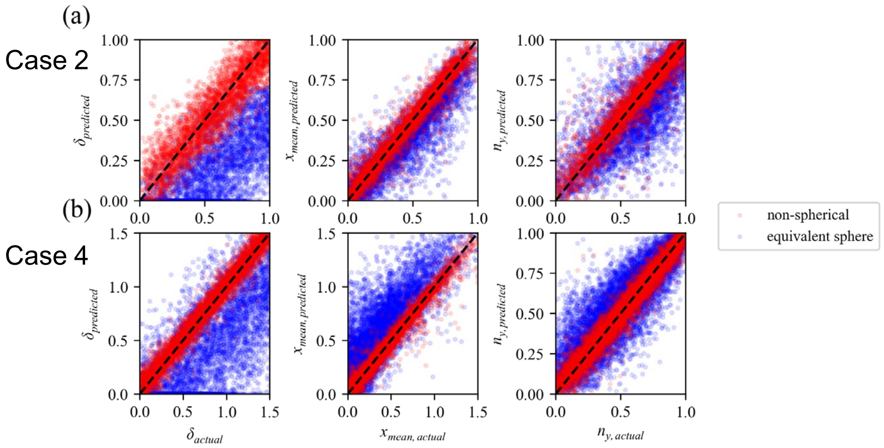

Case	1	2	3	4	5	6
Contact frequency ratio	49.40%	33.50%	33.30%	41.90%	49.50%	59.80%
Accuracy of the detection model	96.70%	96.20%	97.70%	96.80%	97.70%	97.50%
Accuracy assuming spheres	76.80%	76.30%	83.30%	96.60%	91.50%	89.30%
MSEs from the contact model	0.005	0.008	0.0067	0.004	0.0016	0.0045
MSEs assuming spheres	0.0653	0.0626	0.0802	0.0008	0.0204	0.0914
Sphericity	0.92	0.8	0.84	**0.98**	0.91	0.74

Conclusion

- This study provides the interaction force and collision models for the non-spherical particles.
- In DEM, the NN based models can be implemented to obtain the interaction forces and collision forces.
- Both models show high accuracy of prediction on the forces and collision properties.
- The collision model can improve the computation efficiency.

Acknowledgement

Acknowledgment: "This material is based upon work supported by the Department of Energy Award Number DE-FE0031905."